Formation and Function of Organized Gut Associated Lymphoid Tissue in Health and Disease

Olivier, B.J.

2010

Chapter 4

Formation of tertiary lymphoid tissue in dextran sulfate sodium induced colitis is partially dependent on LT$\alpha_1\beta_2$-LTβR axis

B.J. Olivier[1], M. Knippenberg[1], M.J. Greuter[1], G. Goverse[1], E.D. Keuning[1], A.A. te Velde[2], G.Bouma[3] and R.E. Mebius[1].

[1] Department of Molecular Cell Biology and Immunology, Vrije Universiteit Medical Center, Amsterdam, The Netherlands.
[2] Tytgat Institute for Liver and Intestinal Research, Academic Medical Center, Amsterdam, The Netherlands.
[3] Department of Gastroenterology, Vrije Universiteit Medical Center, Amsterdam, The Netherlands.

Manuscript in preparation

Abstract

Patients with inflammatory bowel disease (IBD) suffer from chronic inflammation of the intestine, which may lead to the formation of lymphoid aggregates that closely resemble secondary lymphoid tissue. The formation of secondary lymphoid tissue is dependent on the lymphotoxin alpha1 beta2 - lymphotoxin beta receptor signaling axis. Hematopoietic lymphoid tissue inducer (LTi) cells express lymphotoxin alpha1 beta2 ($LT\alpha_1\beta_2$) which binds to the lymphotoxin beta receptor ($LT\beta R$) expressed on stromal organizers cells, and leads to the induction of chemokines (CXCL13 and CCL21) and adhesion molecules (VCAM-1, ICAM and MAdCAM-1). These molecules serve to attract and retain LTi cells. Here we show, using dextran sulfate sodium (DSS) induced colitis, that stromal cells in the acute inflammatory setting had the ability to upregulate $LT\beta R$ expression along with CXCL13, CCL21, VCAM-1 and MAdCAM-1. In the more chronic setting, tertiary lymphoid tissue was detected in inflamed colons and consisted of tightly clustered B cell follicles with distinct T cell areas. Surprisingly, these structures could also be found at the chronic phase of DSS colitis in $LT\alpha^{-/-}$ mice, although the B cell areas were devoid of follicular dendritic cells (FDCs). These results show that lamina propria stromal cells become activated upon damage to the epithelial barrier and function as organizer cells to locally form lymphoid tissue. This process is only partially dependent on the $LT\alpha_1\beta_2$-$LT\beta R$ axis and must involve alternate pathways.

Introduction

In a variety of chronic inflammatory diseases (i.e. Rheumatoid arthritis, Sjögren syndrome, Myasthenia gravis, Hashimoto thyroiditis, Grave's disease and Multiple sclerosis) lymphocyte infiltrates appear within the chronically inflamed tissue, which exhibit a high degree of cellular organization, and are referred to as tertiary lymphoid tissue [1]. These organized cellular structures strongly resemble secondary lymphoid tissue such as lymph nodes and Peyer's patches (PPs), which are typically organized into distinct B- and T-cells areas, with B cell follicles containing follicular dendritic cells (FDCs) and germinal centres (GCs). Both secondary and tertiary lymphoid tissues have high endothelial venules (HEVs) and lymphatic endothelium [2-5]. The similarities between tertiary lymphoid tissue and secondary lymphoid tissue suggest that the processes involved in the generation and maintenance of these tissues may have common features [3, 4, 6-8]. In embryonic life, the formation of lymph nodes and PPs involves the paracrine triggering of lymphotoxin beta receptor (LTβR) expressed on stromal organizer cells by lymphotoxin alpha1 beta2 ($LT\alpha_1\beta_2$) expressed on hematopoietic lymphoid tissue inducer (LTi) cells. This signaling results in the induction of chemokines (CXCL13, CCL19 and CCL21) and adhesion molecules (ICAM, VCAM-1 and MAdCAM-1) on stromal organizer cells [9]. The increased expression of chemokines and adhesion molecules serves to attract and retain more $LT\alpha_1\beta_2$ expressing LTi cells to the area which subsequently leads to more LTβR triggering. This gives rise to a self sustaining feedback loop which ultimately results in the formation of lymph nodes and PPs [9-13]. There is evidence to support that the formation of tertiary lymphoid tissue is also dependent on the $LT\alpha_1\beta_2$-LTβR signaling axis as transgenic animals which express lymphotoxin under the rat insulin promoter (RIP-LT) form tertiary lymphoid tissue in the kidney and pancreas as a result of ectopic lymphotoxin expression [6].

The healthy adult mouse colon contains a variety of dynamic organized gut associated lymphoid tissues (GALT), namely colonic patches, cryptopatches and isolated lymphoid follicles (ILFs). Colonic patches are thought to be the counterpart of small intestine PPs occurring in the colon. Their formation is programmed in embryonic life and they are thus secondary lymphoid tissue. It has been shown that these structures contain multiple B cell follicles with

distinct T cell areas. They contain lymphatic endothelium, FDCs and GCs (Chapter 2). These structures remain constant in number in an inflammatory setting but expand in size as a response to inflammation within the colon [14]. The formation of colonic patches, similar to the formation of PPs, is dependent on the $LT\alpha_1\beta_2$-LTβR signaling axis. It has been shown that $LT\alpha^{-/-}$ mice and mice that are treated *in utero* with the inhibitory soluble fusion protein for LTβR fail to form colonic patches [15, 16].

In addition to colonic patches, a second type of organized GALT is present in the colon, namely cryptopatches and ILFs. For the small intestine, Pabst *et al* have proposed to group cryptopatches (primarily containing cKit+ cells) and isolated lymphoid follicles (containing cKit+ cells and B lymphocytes) together and collectively refer to them as solitary intestinal lymphoid tissue (SILT). They proposed that SILT can be divided into five different classes depending on size and cellular composition (ratio of c-Kit+ cells versus B lymphocytes) with the smallest SILT containing mostly c-Kit+ cells (also known as cryptopatches) and the larger ones containing mainly B cells (also known as mature ILFs) . SILT forms in the first two weeks after birth and the total number of these structures remains constant in the adult small intestine. They can however remodel in size and cellular composition in response to the microflora present within the lumen but always consist of a single cluster of cells within the lamina propria [17]. More mature SILT in the small intestine have been shown to contain GCs and to be capable of IgA production [18]. For the remainder of this paper both cryptopatches and ILFs will be grouped together and referred to as SILT. The formation of SILT in the small intestine has also been shown to be dependent on the $LT\alpha_1\beta_2$-LTβR signaling axis, since both $LT\alpha^{-/-}$ and $LT\beta R^{-/-}$ mice were reported to lack cryptopatches as well as ILFs [19-21]. Due to the fact that different SILT stadia already exist within the setting of the healthy colon and that these structures expand in size in the inflammatory setting, detection of additional tertiary lymphoid tissue which may form in the colon in response to inflammation has been reported to be difficult [1].

Patients with ulcerative colitis or Crohn's disease, collectively referred to as inflammatory bowel disease (IBD), suffer from chronic inflammation of intestinal tissue and the presence of structured lymphoid aggregates within

the chronically inflamed intestines has been reported [22]. For various chronic inflammatory diseases, a role for the $LT\alpha_1\beta_2$-LTβR signaling pathway in the formation of tertiary lymphoid tissue has been shown, however the mechanism of its involvement is unclear [15, 23]. To investigate the effects of inflammation on lamina propria stromal cells in both the acute and chronic phase use was made of the previously described dextran sulfate sodium (DSS) murine colitis model [24]. The DSS colitis model has been reported to give rise to intestinal inflammation which resembles the human form of ulcerative colitis [25]. DSS is a chemical compound which, upon oral administration, is thought to have toxic effects on the epithelial barrier of the intestine resulting in an alteration of the permeability of the intestine [26]. The increase in intestinal permeability may serve as a means for bacteria present in the large intestine to infiltrate the lamina propria thus evoking an inflammatory response. We show here that DSS administration leads to the activation of stromal cells in the lamina propria of the colon, which start to express the distinguished markers of lymphoid tissue stromal organizer cells i.e. LTβR and VCAM-1. Subsequently, we show that in the chronic phase of the disease a third type of GALT has developed, which can only be found in inflamed colon and which does not comply with the definition of either SILT or colonic patches.

Materials and Methods

Mice

Standard pathogen free C57BL/6 and $LT\alpha^{-/-}$ female mice were obtained form Charles River Laboratories (Maastricht, The Netherlands) and housed in the animal facility at the Vrije Universiteit (Amsterdam, The Netherlands). Animals were housed under standard laboratory conditions with a starting age of 8-10 weeks and a weight range of 18-20 grams. Ethics committee approval was obtained from the Vrije Universiteit Animal Ethics Committee.

Induction of DSS Colitis

Use was made of an acute and chronic DSS colitis model as previously described [24]. Mice were given 2% DSS in drinking water *ad libitum* which was changed on a daily basis. The duration of the experiments was 35 days. Control animals included in the experiments were given normal drinking

water. To induce acute colitis mice were given DSS for the last 7 days of the experiment prior to euthanasia. To induce chronic colitis mice were given DSS for the first 5 days of the experiment after which they received normal drinking water for an additional 30 day period. To assess the severity of the induced colitis at termination colons were measured and mice were assigned an inflammatory and diarrhea score (as defined by Melgar *et al* [24]).

Immunofluoresence

Mice were euthanized, colons were removed and embedded in OCT compound (Sakura Finetek, Europe) and stored at -80^{o}C. Entire colons were serially sectioned on the cryostat (7 microns) and every 20th section was screened for the presence of organized lymphoid tissue by hematoxylin and eosin staining, slides containing infiltrates were subsequently acetone fixed and immunofluoresence stainings were performed. For overview pictures a representative length of colon was visualized by making use of the stitch picture function with a 20x objective of the DM6000 Leica Immunofluoresence Microscope Leica (Leica Microsystems, Rijswijk, The Netherlands). For higher magnification pictures use was made of the Leica TCS-SP2-AOBS Confocal Laser Scanning Microscope (Leica Microsystems).

Antibodies

Anti-glycoprotein 38 (GP38, also known as podoplanin, clone 8.1.1) and anti-CD3 (clone KT3) were used as supernatants and visualized by means of the appropriate secondary antibody labeled with Alexa-Flour 647, Alexa-Flour 488, or Alexa-Flour 546 (Invitrogen Life Technologies, Breda, The Netherlands). Anti-MAdCAM-1 (clone MECA-367), anti-B220 (clone 6B2) and anti-CD35 (clone 8C12) were affinity purified from hybridoma cell culture supernatants with protein G-Sepharose (Pharmacia, Uppsala, Sweden) and labeled with Alexa-Fluor 488 or Alexa-Fluor 647 (Invitrogen). Anti-LTβR (clone 4H8WH2, Alexis Biochemicals, San Diego, CA, USA), anti-CXCL13 (R&D Systems, Minnneapolis, USA), anti-CCL21 (R&D Systems), and anti-VCAM-1 (BD Bioscience, San Jose, CA, USA) were visualized by making use of the TSA signal amplification kit with HRP-streptavidin and Alexa-Fluor 546 tyramide (Invitrogen). Anti-smooth muscle actin (clone 1A4, Sigma-Aldrich, St.

Louis, MO, USA), anti-CD31 (clone ERMP-12, kindly provided by P. Leenen, Erasmus University, Rotterdam), anti-Lyve-1 (Millipore, Billerica, MA, USA) anti-βIII tubulin (clone TUJ1, Covance, Rotterdam, The Netherlands) and anti-ALDH1A1 (also known as RALDH1, Abcam, Cambridge, UK) were visualized by means of the appropriate secondary antibody labeled with Alexa-Flour 488, Alexa-Flour 546, or Alexa-Flour 647 (Invitrogen Life Technologies).

Quantitative Real time RTPCR

Whole colons were removed, placed in TRIZOL (Invitrogen) and stored at -80 °C. Whole colons were homogenized and RNA was isolated as per manufacturer's instruction. The concentration of RNA was assessed by means of the Nanodrop Spectrophotometer (Nanodrop Technologies, Wilmington, DE). cDNA was synthesized by making use of a reverse transcriptase reaction which was performed according to the MBI Fermentas cDNA synthesis kit (Fermentas, Vilnius, Lithuania), using both the Oligo(dT)18 and the D(N)6 primers. Quantitative real time RTPCR was performed on the ABI Prism 7900 Sequence Detection System (Applied Biosystems, Foster City, CA). The reactions were performed with 0.25ng cDNA in a total volume of 10 µl containing SYBR Green PCR Master Mix (Applied Biosystems, Foster City, CA) and 300 nM of each primer as per manufacturer's instructions. Primers were designed using Primer Express Software (Applied Biosystems) according to the guidelines provided by the manufacturer (Table 1).

Statistical Analysis

Data obtained by quantitative real time PCR were normalized for the geometric mean of the two most stable house-keeping genes (cyclophilin, ubiquitin) as determined by analysis with geNorm method software (http://medgen.ugent.be/~jvdesomp/genorm/). For both real time PCR and macroscopic colitis scores a two-tailed unpaired student's t-test was used to analyse differences between groups with * significant, if $p<0.05$; ** significant, if $P<0.01$; *** significant, if $p<0.001$.

Primer	Sequence 5' --> 3'
Cyclophilin Forward Reverse	 ACC CAT CAA ACC ATT CCT TCT GTA TGA GGA AAA TAT GGA ACC CAA AGA
Ubiquitin Forward Reverse	 AGC CCA GTG TTA CCA CCA AG ACCCAAGAACAAGCACAAGG
CD45 Forward Reverse	 CCC CGG GAT GAG ACA GTT G AAA GCC CGA GTG CCT TCC T
CD19 Forward Reverse	 GTG CTC TCC CTT CCT ACA TC CTG ACC TTC TTC TTC CCC TC
CD3 Forward Reverse	 GTG GCT ACT ACG TCT GCT AC TGG ACT GTC GTC ATC GGT ATT
CXCL13 Forward Reverse	 CAT AGA TCG GAT TCA AGT TAC GCC TCT TGG TCC AGA CAC AAC TTC A
CCL21 Forward Reverse	 GCT GCA AGA GAA CTG AAC AGA CA CGT GAA CCA CCC AGC TTG A

Table 1 - Primer sequences used in the study for real time RT-PCR

Results

Induction of Acute and Chronic Colitis

To follow the formation of tertiary lymphoid tissue during the course of colitis inflammation was induced in the colon by administering DSS in drinking water and colons were analyzed at the acute or chronic phase of the disease. As weight loss is associated with the progression of colitis all mice included in the experiments were weighed on a daily basis. To determine the effects of acute inflammation on the tissue, acute colitis was induced by administering DSS on the last 7 days of the experiment prior to euthanasia. Daily weight graphs for these mice show a progressive weight loss in these animals during the DSS administration period with acute colitis mice weighing significantly less when compared to age matched controls at day 34 and 35 (Figure 1A). To induce chronic inflammation, DSS was administered for the first 5 days of the experiment followed by a consecutive 30 day period on normal drinking water [24]. In the chronic DSS model, mice had significantly lower weights from day 8 until day 10 when compared to the age matched control group, followed by a weight recovery phase (Figure 1B). The measurement of colon length shows that the acute colitis mice have significantly shorter colons when compared to controls. This significant reduction in length is still present in the chronic colitis group confirming that these mice have not yet fully recovered from the DSS induced colitis (Figure 1C). Both at the acute and chronic phase of colitis inflammation could be observed in the colons at termination (Figure 1D). Furthermore, the diarrhea score supports the previous two macroscopic scores and confirms that indeed colitis is present in these animals at termination (Figure 1E). Analysis by real time RTPCR revealed that mRNA for the marker CD45 was increased in colons of acute and chronic colitis animals, indicating an influx of hematopoietic cells into the inflamed colons (Figure 2A). Further analysis revealed a significant increase of B cells (CD19) but not T cells in the colons of mice with chronic colitis (Figure 2B and 2 C).

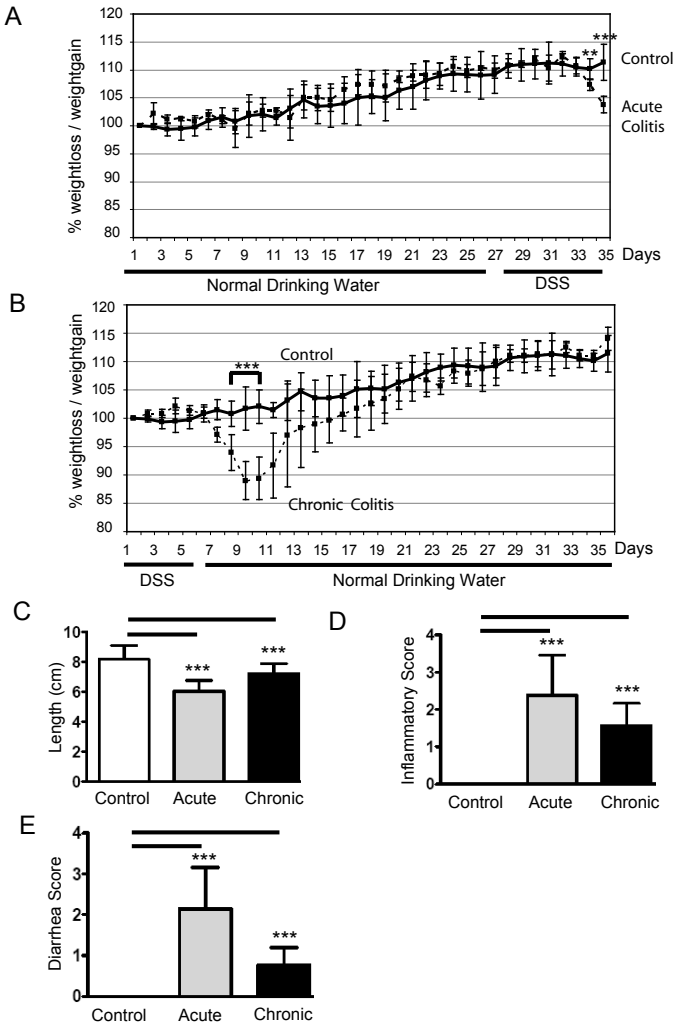

Figure 1 – Daily changes in body weight and macroscopic scoring of DSS induced colitis

(A) Daily weight graphs for control and acute colitis animals included in the experiments (average +/- SD). Control mice received normal drinking water throughout the experiment and the acute colitis group received 2% DSS in drinking water for the last seven days of the experiment. (B) Daily weight graphs for control and chronic colitis animals included in the experiments (average +/- SD). Control mice received normal drinking water throughout the experiment while the chronic colitis mice received 2% DSS in drinking water for the first 5 days of the experiment and then normal drinking water for the next 30 days. Results are representative of 7 animals per group with 3 repeats. Significant p values are indicated with * ($p<0.01$ ** and $p<0.001$ ***). (C) Shows colon length in cm (average +/- SD) of mice included in the experiments. (D) Shows inflammatory score (average +/- SD). (E) Shows diarrhea score (average +/- SD). Significant p values indicated with *** $p < 0.001$. All averages are representative of 7 mice per group with 3 repeats.

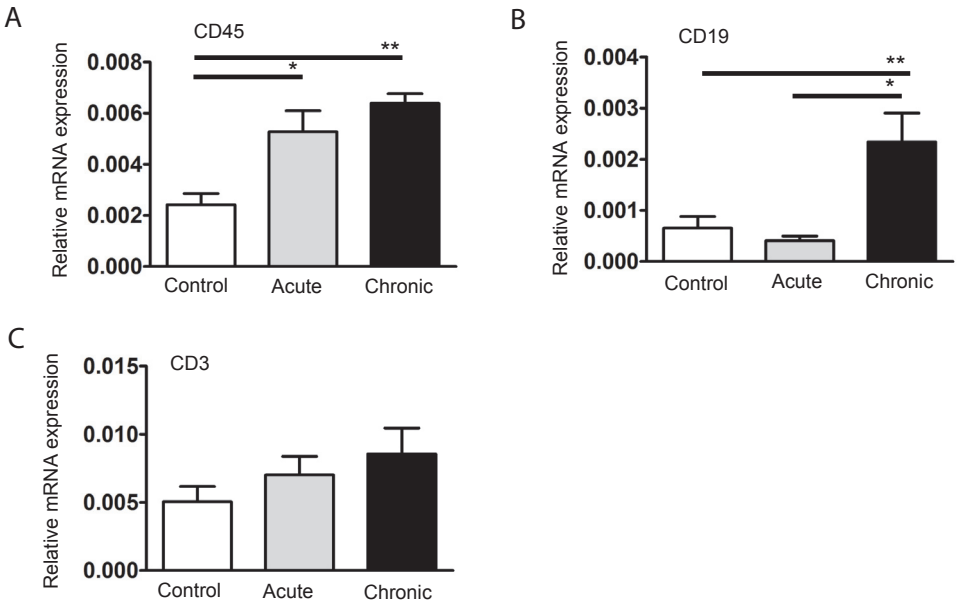

Figure 2 – Influx of lymphocytes in acute and chronic inflammation
Real time RT-PCR analysis showing relative mRNA expression levels (average +/-SD) of (A) CD45, (B) CD19 and (C) CD3 whole colon of healthy controls, acute and chronic DSS colitis. Significant p values are indicated with * ($p<0.05$ * and $p<0.01$ **).

Lamina propria stromal cells become activated at place of ulceration

It is known that triggering of LTβR on stromal organizer cells is responsible for the definitive formation of secondary lymphoid tissue during development [27].

To see whether LTβR triggering could contribute to the influx of hematopoietic cells in the colon we performed immunofluoresence stainings to determine whether LTβR was expressed on stromal cells in the lamina propria of the colon. Within healthy colons the presence of a GP38 $^{+}$ stromal cell network which runs throughout the lamina propria of the colon was observed. However these stromal cells showed little to no LTβR expression (Figure 3A). Interestingly, stromal cells in the areas of ulceration of acutely inflamed colons showed an increased expression of LTβR only within affected areas (Figure 3B). Triggering of LTβR on stromal organizer cells during ontogeny is known to cause an induction of CXCL13. Analysis of CXCL13 showed that very few stromal cells in the healthy colon express CXCL13 (Figure 3C).

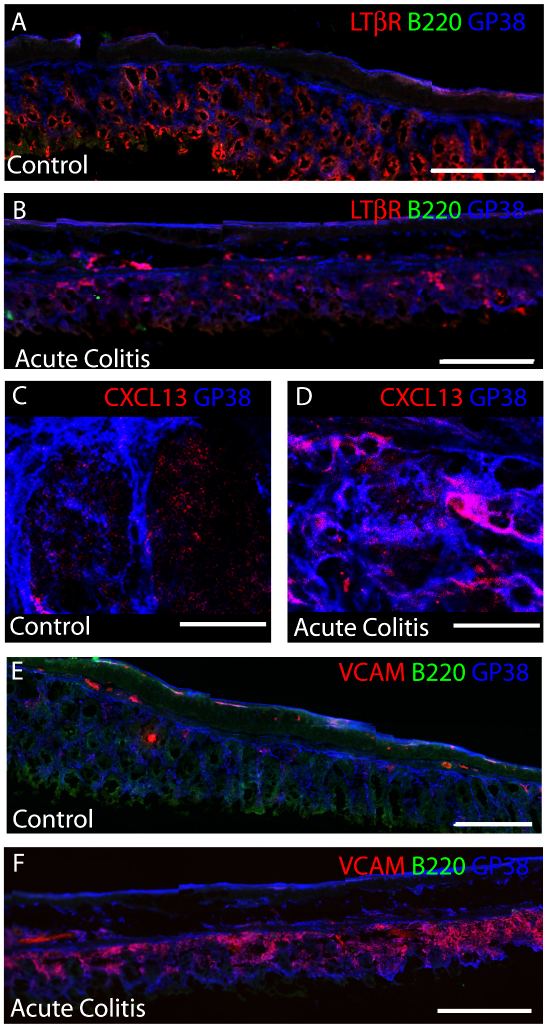

Figure 3 – Activation of stromal cells in the acutely inflamed colon

Immunofluoresence analysis of stromal cell network in control (A, C and E) and acute DSS colitis (B, D and F) mice. (A) Shows a representative overview of stromal cells which express little to no LTβR in control colon. (B) Representative overview of stromal cells which upregulate LTβR in acute colitis (LTβR in red and GP38 in blue, scale bars represent 250 μm). (C) Shows low levels of CXCL13 produced by stromal cells in control colons. (D) Shows an increased level of CXCL13 by stromal cells in acutely inflamed colons (CXCL13 in red and GP38 in blue, scale bars represent 50 μm). (E) Shows representative overview of little to no expression of VCAM-1 by stromal cells in control colons. (F) Shows up regulation of VCAM-1 by stromal cells (VCAM-1 in red and GP38 in blue, scale bars represent 250 μm) in acute colitis. All pictures were taken on DM6000 Leica Immunofluorescence Microscope Leica (Leica Microsystems). (A, B, E and F) Representative overviews of colonic tissue were taken with 20x magnification stitch picture function and (C and D) relevant area of interest of colon.

However, in the acute inflammatory settings stromal cells showed an increased expression of CXCL13 (Figure 3D). The triggering of LTβR is also known to cause an upregulation of the adhesion molecule (VCAM-1) which is responsible for the retention of hematopoietic cells during secondary lymphoid tissue formation. In the healthy setting there was little to no expression of VCAM-1 on stromal cells of the lamina propria (Figure 3E). In the acute inflammatory setting, a remarkable induction of VCAM-1 expression on stromal cells within the area of ulceration was observed (Figure 3F). Both CXCL13 and VCAM-1 may serve in the adult colon to attract and retain lymphocytes, respectively. Upon analysis of the acute colitis time point a diffuse influx of T and B cells were indeed observed in the areas of ulceration however no clustering of these cells could be seen (data not shown). Thus taken together, stromal cells present in the areas of inflammation of the colon show characteristics of stromal organizers cells by expression of LTβR and their ability to produce chemokines and express adhesions molecules. These molecules may serve to attract and retain lymphocytes to the inflamed area, which could potentially result in the formation of tertiary lymphoid tissue.

Formation of Tertiary Lymphoid Tissue in Chronic Colitis

In the healthy colon two different organized GALT structures have been reported to exist i.e. SILT and colonic patches. In chronically inflamed colons we observed that SILT and colonic patches had increased in size and that these structures were often macroscopically visible upon dissection of the colons. Despite the expansion of SILT in the chronic inflammatory setting, immunofluoresence analysis revealed that these SILT remained as single clusters of B cells with scattered T cells, while colonic patches contained more than one B cell follicle with distinct T cell areas (Figure 4A). Furthermore, these two structures occurred in different locations in the colon with the SILT located in the lamina propria and colonic patches located in the submucosa of the colon (Figure 4B). Thus despite the expansion of these two organized GALT structures they could still be identified on grounds of the number of B cell follicles, the presence of a distinct T cell areas and their anatomical location.

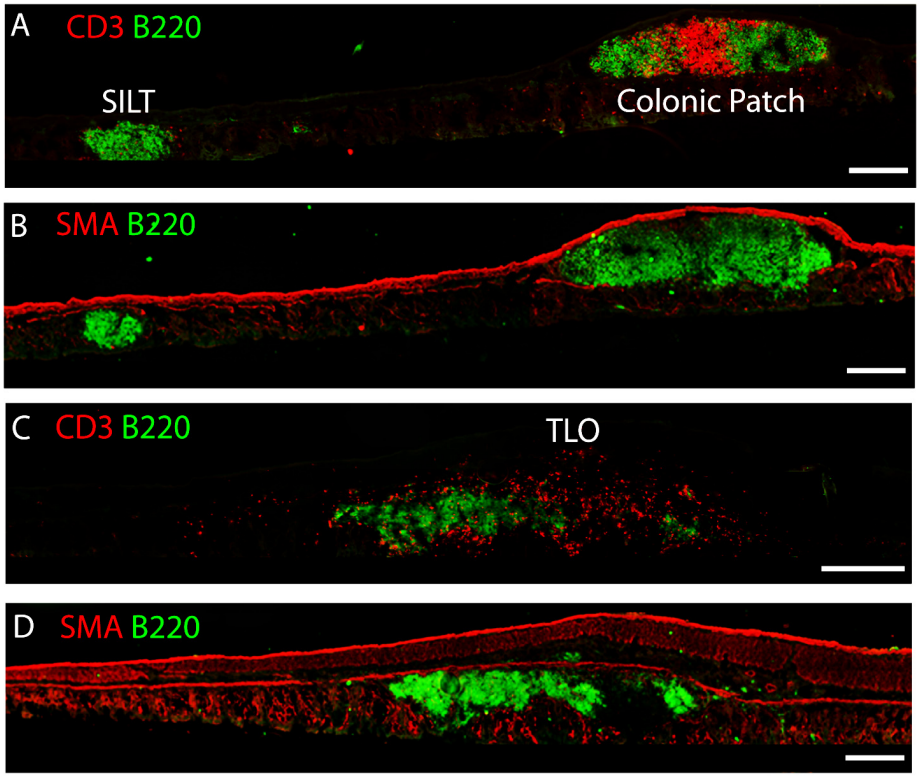

Figure 4 – Characterization of tertiary lymphoid tissue in chronically inflamed colon
Microscopic examination of organized GALT and tertiary lymphoid tissue in chronically inflamed colons. (A) Shows a representative example of SILT and a colonic patch present in the chronic inflammatory setting. SILT structures consists of a single B cell follicle with a few randomly scattered T cell whereas the colonic consists of more than one B cell follicle with a distinct T cell micro-domain (B220 in green and CD3 in red) (B) Smooth muscle actin stains the muscle layers of the colon and illustrates that the B cell follicle of the SILT occurs in the lamina propia whereas the colonic patch occurs in the sub mucosa (B220 in green and SMA in red). (C) Shows a third organized GALT structure which consists of more than one B cell follicle with a diffuse T cell area (B220 in green and CD3 in red). These structures are not observed in control colons but are observed in chronically inflamed colon +/- 3 structures per colon. (D) These structures are present in the lamina propria of the colon and do not occur between the two muscle layers (B220 in green and SMA in red). All pictures were taken of a representative length of tissue on the 20x magnification on stitch picture function DM6000 Leica Immunoflourescence Microscope Leica (Leica Microsystems) with scale bars representing 250 μm.

In the chronic inflammatory setting a third type of organized GALT structure was detected which did not comply with the definition of either SILT or colonic patches. These structures consisted of more than one loosely clustered B cell area which were separated by distinct T cell areas (Figure 4C) and located in the lamina propria of the colon (Figure 4D).

These B cell follicles (Figure 5A) contained stromal cells expressing LTβR, CXCL13 and VCAM-1 (Figure 5B - D). The expression of CXCL13 could potentially serve to attract B cells to the area while the expression of VCAM-1 could serve to retain lymphocytes within these areas. Since distinct T cell areas could be observed one would expect a T cell attracting chemokine to be expressed within the inflamed areas. CCL21 is a major T cell attracting chemokine which is expressed in the T cell areas of secondary lymph nodes [28, 29]. Indeed, immunofluoresence staining revealed a network of lymphatic endothelium extending throughout the colon which expressed CCL21 (Figure 5E).

To determine to what level the multifollicular structures in the lamina propria were developed we addressed whether the B cell follicles contained CD35 expressing follicular dendritic cells (FDCs) and specialised HEVs. Indeed, immunofluoresence stainings revealed that the multifollicular B cell structures in the lamina propria, which are only found in chronically inflamed colons, indeed contained FDCs (Figure 6A and B). These organized GALT structures also had a $CD31^+$ vascular network occurring throughout the structures. Furthermore, MAdCAM-1 was expressed on blood vessels, with a cuboidal appearance, suggesting the presence of MAdCAM-1^+ HEVs (Figure 6C and D).

Since these multi-follicular structures had distinct T cell areas, occurred in the lamina propria, contained FDCs as well as HEVs and were only present in chronically inflamed colons we propose that these structures are indeed true tertiary lymphoid tissue. These structures are therefore referred to as such in the remainder of the text.

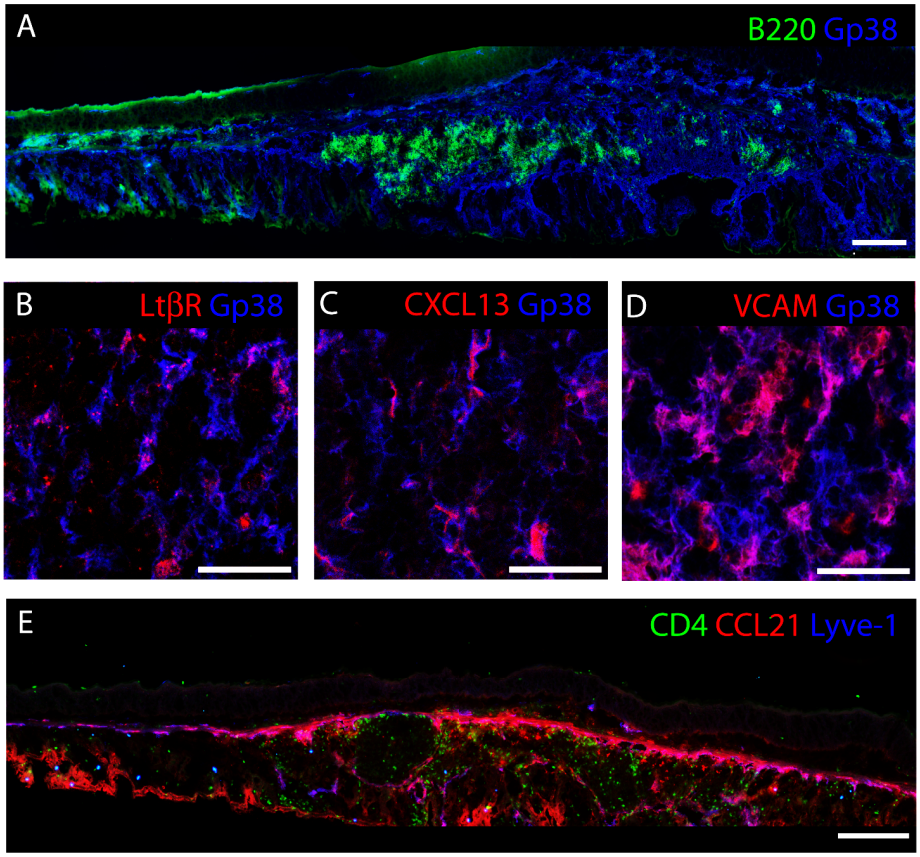

Figure 5 – Increased expression of chemokines and adhesion molecules within tertiary lymphoid tissue of chronically inflamed colon

(A) Representative overview of B cell follicles which form in chronically inflamed colon which contain a stromal cell network (B220 in green and podoplanin/ gp38 in blue, scale bar = 250 μm). (B, C and D) Increased expression of LTβR, CXCL13 and VCAM respectively by stromal cells within TLO (marker of interest in red and podoplanin / gp 38 in blue, scale bars = 50 μm). (E) Representative overview of lymphatic endothelium of chronically inflamed colon which provides a sourc of CCL21 which occurs in close association with the T cell area of the tertiary lymphoid tissue (CD 4 in green, CCL21 in red and Lyve-1 in blue, scale bar = 250 μm). (A and E) Representative length of tissue on the 20x magnification on stitch picture function DM6000 Leica Immunoflourescence Microscope Leica (Leica Microsystems) (B, C and D) Zoom in of stromal cells within B cell follicle of TLO taken on the Leica TCS-SP2-AOBS Confocal Laser Scaninning Microscope (Leica Microsystems).

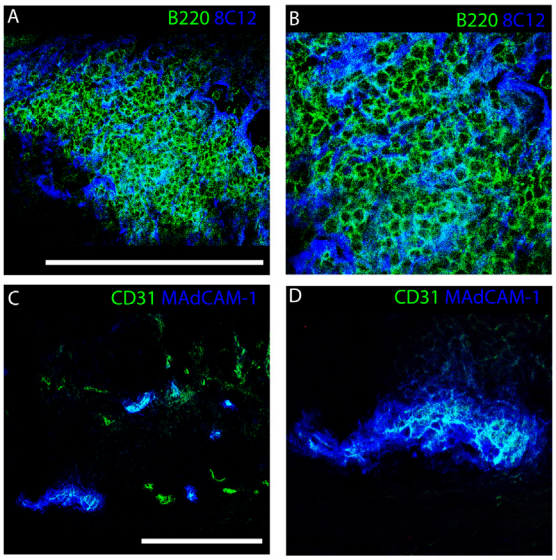

Figure 6 – Tertiary lymphoid tissue contains FDCs and HEVs

(A and B) B cell follicle in the lamina proria area from potential tertiary lymphoid tissue does indeed contain follicular dendritic cells (FDCs)(CD45R+ in green, and CD35 in blue, scale bars = 50 μm). (C and D) These structures also contain endothelium which expresses MAdCAM indicating that these vessels are indeed HEVs (CD31+ in green and MAdCAM-1 in blue, scale bars = 50 μm). All pictures were taken on the Leica TCS-SP2-AOBS Confocal Laser Scaninning Microscope (Leica Microsystems). Picture A and C taken on a 40x objective, picture B and D increased magnification of the area of interest.

Formation of Tertiary Lymphoid Tissue is partially dependant on LTα$^{-/-}$ in Chronic Colitis

To determine if the formation of tertiary lymphoid tissue in chronic colitis is indeed dependent on the LT$\alpha_1\beta_2$-LTβR axis chronic DSS colitis was induced in LTα$^{-/-}$ animals. Surprisingly, microscopic analysis confirmed that tertiary lymphoid tissue like structures were present in the chronically inflamed colon consisting of more diffuse B- and T- cell infiltrates (Figure 7A). These structures were found within the lamina propria of the inflamed colon and are thus found in a similar position as the tertiary lymphoid tissue that was observed in wild type mice (Figure 7B). We have previously shown during embryonic development that retinoic acid, possibly derived from neurons, can have a direct effect on stromal organizer cells (Chapter 3). Retinoic acid, which is the active metabolite of vitamin A, can cause a LT$\alpha_1\beta_2$-LTβR independent induction of CXCL13 by stromal organizers cells (Chapter 3).

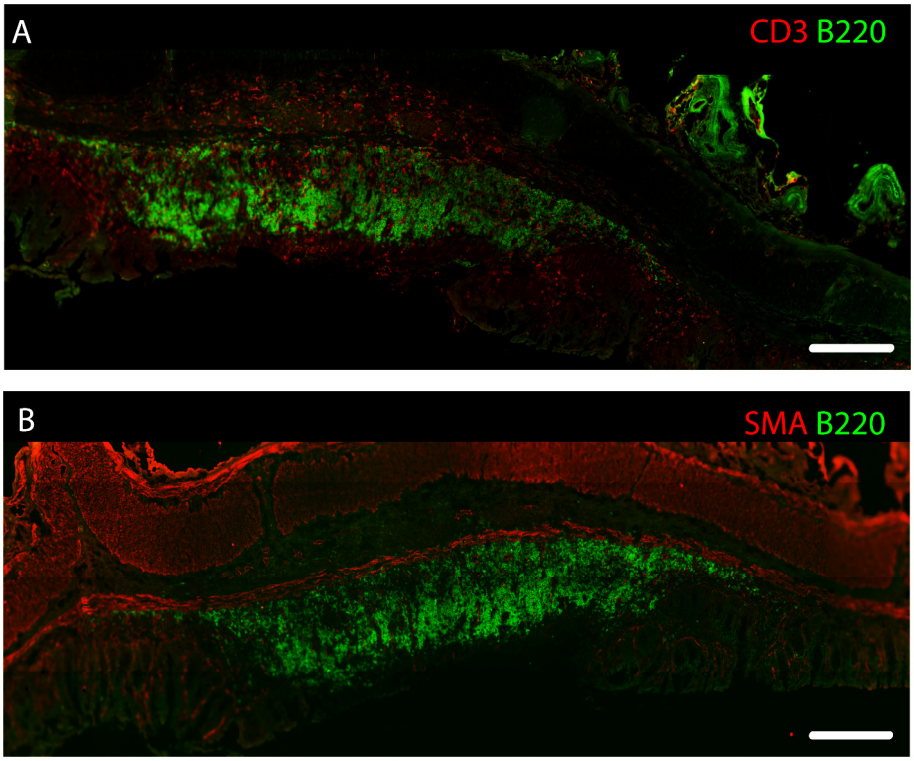

Figure 7 – Formation of tertiary lymphoid tissue like structures in chronically inflamed Ltα $^{-/-}$ colons

(A) Representative overview of diffuse B cell clusters with distinct T cell area occurring in Ltα $^{-/-}$ colon (B220 in green and CD3 in red). (B) Tertiary lymphoid tissue like structure like the tertiary lymphoid tissue formed in C56BL/6 mice occurs in the lamina propria of the chronically inflamed colon (B220 in green and SMA in red). Representative length of tissue on the 20x magnification on stitch picture function DM6000 Leica Immunoflourescence Microscope Leica (Leica Microsystems) with scale bars representing 250 μm.

To see whether an LTα independent induction of CXCL13 could be measured in the inflamed colon, real time RTPCR analysis was performed to quantify mRNA levels of CXCL13. In both the acute and chronic inflammatory setting in wild type mice we could measure a significant upregulation of the B cell attracting chemokine CXCL13 (Figure 8A). However, no such induction of CXCL13 was observed in LTα$^{-/-}$ animals in either the acute or chronic inflammatory setting (Figure 8B). As this analysis was performed on whole colon homogenates we reasoned that subtle differences in CXCL13 would

not be detected. We therefore subsequently used immunofluorescence to address whether CXCL13 on stromal cells could be detected within the B cell area of the tertiary lymphoid like tissue in these animals. Indeed CXCL13 expression in stromal cells within tertiary lymphoid tissue was observed, indicating a $LT\alpha_1\beta_2$-LTβR independent upregulation of CXCL13 in $LT\alpha^{-/-}$ animals (Figure 8C).

To support the hypothesis that a neuronal source of retinoic acid may be responsible for the $LT\alpha_1\beta_2$-LTβR independent induction of CXCL13 we performed immunofluoresence stainings for a general neuronal marker (βIII-tubulin) in combination with an enzyme (RALDH) which is known to convert vitamin A into its active metabolite retinoic acid. Indeed we show that nerves which express RALDH were present within the tertiary lymphoid tissues of both wild type (Figure 8D and E) and $LT\alpha^{-/-}$ mice (Figure 8F and G).

Furthermore, analysis of the T cell attracting chemokine CCL21 revealed a significant increase in the acute and chronic inflammatory setting in wild type mice (Figure 9A). In addition, also CCL21 expression in $LT\alpha^{-/-}$ mice was increased in the chronic inflammatory setting compared to control (Figure 9B). Analysis by immunofluoresence confirmed that lymphatic endothelium was present within the tertiary lymphoid tissue like structure in $LT\alpha^{-/-}$ and could therefore serve as a source of CCL21 (Figure 9C). Thus the upregulation of CCL21 in response to chronic inflammation appeared to be independent of LTα.

The B cell areas in the tertiary lymphoid tissue in $LT\alpha^{-/-}$ animals appeared to be more diffuse than those observed in wild type mice. Indeed, these diffuse B cell clusters did not contain FDCs which have been reported to depend on LTβR signaling [30] (figure 10A and B). Surprisingly, further analysis of tertiary lymphoid tissue like structures revealed that $LT\alpha^{-/-}$ do contain HEVs (figure 10C and D). Thus despite the fact that $LT\alpha^{-/-}$ animals can form diffuse B cell follicles and T cell areas and contain HEVs they lack FDCs and can thus not be classified as fully developed tertiary lymphoid tissue. This indicates the partial dependence of the $LT\alpha_1\beta_2$-LTβR signaling axis in the formation of tertiary lymphoid tissue in the chronic inflammatory setting of the colon.

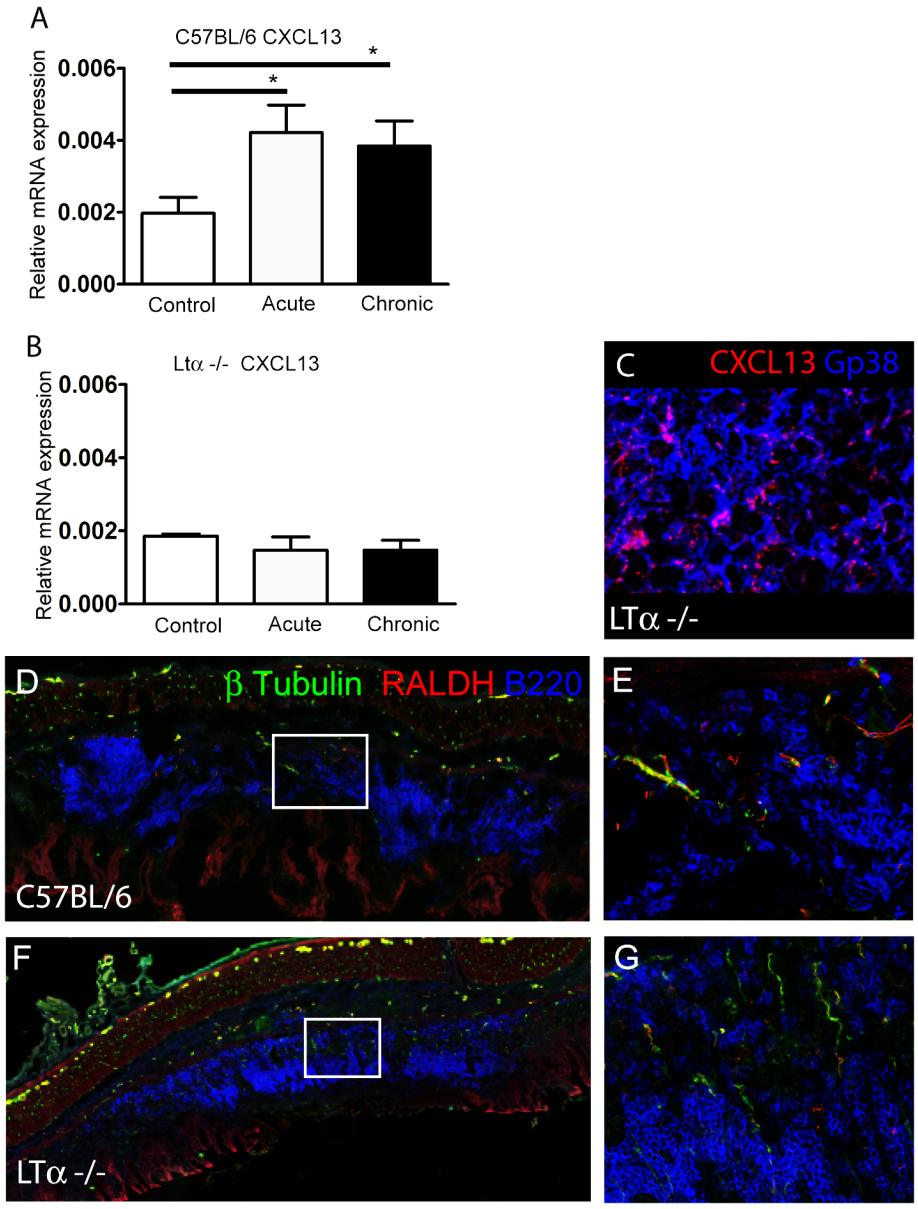

Figure 8 – Expression of CXCL13 can still be observed in the absence of LTα

(A and B) Real time analysis of whole colons showing the relevant mRNA expression levels (average +/-SD) of CXCL13 in C57BL/6 and LTα$^{-/-}$ mice. Significant p values are indicated with p<0.05 *.

(C) CXCL13 expression by stromal cells in tertiary lymphoid like tissue of LTα$^{-/-}$ mice (CXCL13 in red and GP38 in blue). (D-G) Neurons, which produce RALDH, are present within tertiary lymphoid tissue of wild type mice (D and E) and LTα$^{-/-}$ mice (F and G) (β III tubulin in green, RALDH in red and B200 in blue).

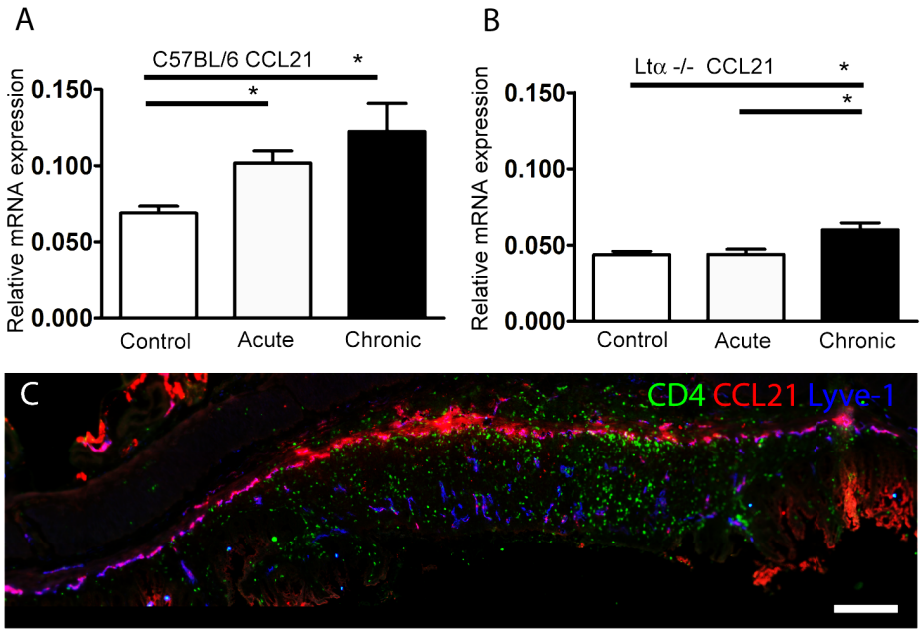

Figure 9 - Increased expression of CCL21 is independent of LTα

(A and B) Real time analysis of whole colons showing mRNA expression levels (average +/-SD) of CCL21 in C57BL/6 and LT$\alpha^{-/-}$ mice. (C) Shows representative overview of tertiary lymphoid tissue like structure in chronically inflamed colon of LT$\alpha^{-/-}$ confirming the upregulation of CCL21 by lymphatic endothelium occurring in close association with the T cell area of the tertiary lymphoid tissue like structure (CD4 in green, CCL21 in red and Lyve-1 in blue). Representative length of tissue taken with a 20x magnification on stitch picture function DM6000 Leica Immunofluorescence Microscope Leica (Leica Microsystems) with scale bars representing 250 μm.

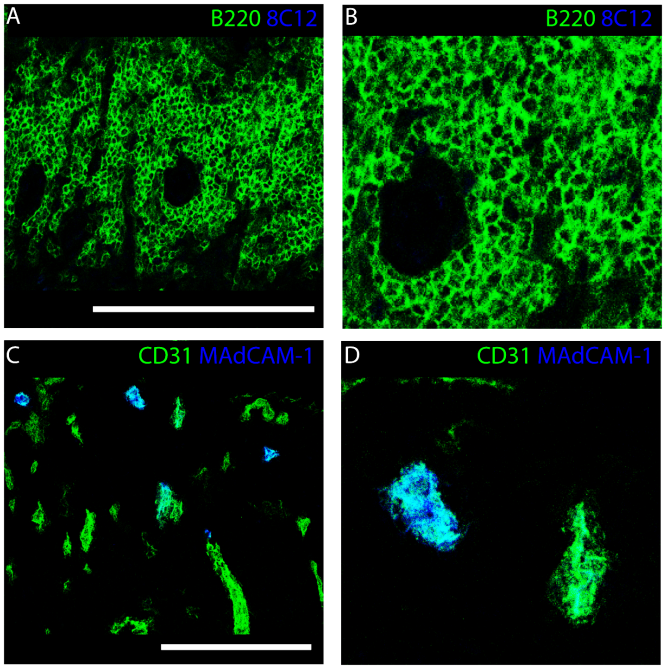

Figure 10 – Tertiary lymphoid tissue like structures in LT$\alpha^{-/-}$ chronic colitis lack FDCs but do contain HEVs

(A and B) Potential tertiary lymphoid tissue in the lamina proria of LT$\alpha^{-/-}$ contains diffuse B cell clusters which do not contain FDCs (B220 in green and CD35 in blue, scale bars = 50 μm). (C and D) However tertiary lymphoid tissue do contain endothelium which expresses MAdCAM-1 indicating that these vessels are indeed HEV's (CD31+ in green and MAdCAM-1 in blue, scale bars = 50 μm). All pictures were taken on the Leica TCS-SP2-AOBS Confocal Laser Scaninning Microscope (Leica Microsystems). Picture A and C taken on a 40x objective, picture B and D increased magnification of the area of interest.

Discussion

Due to the complex and diverse nature of organized GALT present in healthy colon the characterization of newly formed tertiary lymphoid tissue versus secondary lymphoid tissue within the inflamed colon is a challenging task [1]. It has been shown by ourselves and others that SILT and colonic patches are present in the healthy colon and that these structures can expand during inflammation, while the numbers stay constant [14, 17]. SILT by definition consists of a single B cell follicle with a few scattered T cells and is present in the lamina propria of the colon. Colonic patches by definition consist of more than one B cell follicle with a distinct T cell area and form in the submucosa of

the colon. In this study, we have found a novel third type of organized GALT which is only present in chronically inflamed colons and does not comply with the definition of either SILT or colonic patches. These structures consist of more than one B cell follicle with distinct T cell areas and occur in the lamina propria of the inflamed colon. Furthermore these structures contain HEVs and FDCs which are typically characteristics of highly organized lymphoid organs. We propose that this novel third type of organized GALT indeed classify as tertiary lymphoid tissue. Due to the fact that numerous organized GALT is present in the colon, confusion may arise with regards to these structures especially during chronic inflammation. Dohi *et al* has reported that no colonic patches were observed in BALB/c mice treated with LtβR-Ig *in utero* with TNBS induced colitis [15]. However Sphan *et al* reported an increase in colonic lymphoid patches in both LTα$^{-/-}$ and LTβR-Ig *in utero* treated animals on a C57BL/6 background with DSS induced colitis [16]. The discrepancy of the reported findings could be due to strain differences, type of method used to induce colitis or the possibility that the colonic patches observed in DSS colitis were in fact tertiary lymphoid tissue which formed in the inflamed lamina propria as opposed to colonic patches which occur in the submucosa and are present at birth. Thus it is essential to form strict definitions for the three types of organized GALT structures which are present in the colon to avoid subsequent confusion in the literature.

It has been reported that inducible bronchus-associated lymphoid tissue (iBALT), which is tertiary lymphoid tissue that forms in the lungs due to inflammation induced by influenza virus, can form in a lymphotoxin independent manner [31]. These iBALT structures, when present in LTα $^{-/-}$ animals, were shown to contain CXCL13 and CCL21, T cell areas and B cell follicles which lack FDCs. The formation of these iBALT structures indicate that a lymphotoxin independent pathway exists for the formation of tertiary lymphoid tissue. In this paper we show similar findings with regards to the formation of tertiary lymphoid tissue in the context of the chronically inflamed colon. A network of stromal cells is present in the colon, which have the ability to upregulate LTβR upon exposure to inflammation. In addition, these stromal cells have the ability to upregulate key molecules which are known to be dependent on LT$\alpha_1\beta_2$-LTβR signaling, such as CXCL13 and VCAM-1.

This indicates the potential importance of the $LT\alpha_1\beta_2$-LTβR signaling axis in the formation of tertiary lymphoid tissue in the colon. However, $LT\alpha^{-/-}$ have the ability to form tertiary lymphoid tissue like structures suggesting that activation of stromal cells can occur independently of LTβR signaling. The stromal cells within these structures do show the ability to produce CXCL13 in a lymphotoxin independent manner. Immunofluoresence analysis of tertiary lymphoid tissue in both wild type and $LT\alpha^{-/-}$ mice reveals the presence of neurons, within these structures, which express vitamin A converting enzymes and are thus capable of providing retinoic acid to surrounding stromal cells. We have previously shown, in the context of secondary lymphoid tissue formation, that retinoic acid, potentially derived from neurons, can lead to the induction of CXCL13 by stromal cells in a lymphotoxin independent manner (Chapter 3). This suggests that a similar lymphotoxin independent mechanism of tertiary lymphoid tissue formation may play a role in the inflamed colon. However, these structures lack FDCs and are less organized compared to wild type mice. This suggests that LTβR is needed for full organization of these structures. As we see that $CD3^+$ cells are situated around lymphatic endothelium which provides a source of CCL21, in both wild type and $LT\alpha^{-/-}$ mice, we propose that lymphatic endothelium plays an important role in the attraction of T cells in a lymphotoxin independent manner. We therefore propose that upon damage of the colonic epithelial barrier microflora will enter the lamia propria of the colon. This will not only attract hematopoietic cells to this region, but also activate lamina propria cells. Microflora may directly trigger the stromal cells to upregulate a variety of key molecules such as LTβR and VCAM, but perhaps also CXCL13 and CCL21 which serve to attract and retain T and B cells. In addition, also nerve fibers that are attracted to this region may contribute to the lymphotoxin independent formation of tertiary lymphoid structures. The formation of tightly clustered B cell follicles, containing FDCs, in tertiary lymphoid tissue however does require the $LT\alpha_1\beta_2$-LTβR signaling axis.

Reference List

1. Aloisi F, Pujol-Borrell R: Lymphoid neogenesis in chronic inflammatory diseases. Nat Rev Immunol 2006;6:205-217.

2. Weninger W, Carlsen HS, Goodarzi M, Moazed F, Crowley MA, Baekkevold ES, Cavanagh LL, von Andrian UH: Naive T cell recruitment to nonlymphoid tissues: a role for endothelium-expressed CC chemokine ligand 21 in autoimmune disease and lymphoid neogenesis. J Immunol 2003;170:4638-4648.

3. Cupedo T, Mebius RE: Role of chemokines in the development of secondary and tertiary lymphoid tissues. Semin Immunol 2003;15:243-248.

4. Drayton DL, Liao S, Mounzer RH, Ruddle NH: Lymphoid organ development: from ontogeny to neogenesis. Nat Immunol 2006;7:344-353.

5. Finke D, Schmutz S: Interleukin 7-induced lymphoid neogenesis in arthritis: recapitulation of a fetal developmental programme? Swiss Med Wkly 2008;138:500-505.

6. Kratz A, Campos-Neto A, Hanson MS, Ruddle NH: Chronic inflammation caused by lymphotoxin is lymphoid neogenesis. J Exp Med 1996;183:1461-1472.

7. Gommerman JL, Browning JL: Lymphotoxin/light, lymphoid microenvironments and autoimmune disease. Nat Rev Immunol 2003;3:642-655.

8. Newberry RD: Intestinal lymphoid tissues: is variety an asset or a liability? Curr Opin Gastroenterol 2008;24:121-128.

9. Honda K, Nakano H, Yoshida H, Nishikawa S, Rennert P, Ikuta K, Tamechika M, Yamaguchi K, Fukumoto T, Chiba T, Nishikawa SI: Molecular Basis for Hematopoietic/Mesenchymal Interaction during Initiation of Peyer's Patch Organogenesis. J Exp Med 2001;193:621-630.

10. Rennert PD, Browning JL, Mebius R, Mackay F, Hochman PS: Surface lymphotoxin alpha/beta complex is required for the development of peripheral lymphoid organs. J Exp Med 1996;184:1999-2006.

11. Adachi S, Yoshida H, Kataoka H, Nishikawa S: Three distinctive steps in Peyer's patch formation of murine embryo. Int Immunol 1997;9:507-514.

12. Dejardin E, Droin NM, Delhase M, Haas E, Cao Y, Makris C, Li ZW, Karin M, Ware CF, Green DR: The lymphotoxin-beta receptor induces different patterns of gene expression via two NF-kappaB pathways. Immunity 2002;17:525-535.

13. Mebius RE: Organogenesis of lymphoid tissues. Nat Rev Immunol 2003;3:292-303.

14. Dohi T, Fujihashi K, Rennert PD, Iwatani K, Kiyono H, McGhee JR: Hapten-induced colitis is associated with colonic patch hypertrophy and T helper cell 2-type responses. J Exp Med 1999;189:1169-1180.

15. Dohi T, Rennert PD, Fujihashi K, Kiyono H, Shirai Y, Kawamura YI, Browning JL, McGhee JR: Elimination of colonic patches with lymphotoxin beta receptor-Ig prevents Th2 cell-type colitis. J Immunol 2001;167:2781-2790.

16. Spahn TW, Herbst H, Rennert PD, Lugering N, Maaser C, Kraft M, Fontana A, Weiner HL, Domschke W, Kucharzik T: Induction of colitis in mice deficient of Peyer's patches and mesenteric lymph nodes is associated with increased disease severity and formation of colonic lymphoid patches. Am J Pathol 2002;161:2273-2282.

17. Pabst O, Herbrand H, Friedrichsen M, Velaga S, Dorsch M, Berhardt G, Worbs T, Macpherson AJ, Forster R: Adaptation of solitary intestinal lymphoid tissue in response to microbiota and chemokine receptor CCR7 signaling. J Immunol 2006;177:6824-6832.

18. Glaysher BR, Mabbott NA: Isolated lymphoid follicle maturation induces the development of follicular dendritic cells. Immunology 2007;120:336-344.

19. De TP, Goellner J, Ruddle NH, Streeter PR, Fick A, Mariathasan S, Smith SC, Carlson R, Shornick LP, Strauss-Schoenberger J, .: Abnormal development of peripheral lymphoid organs in mice deficient in lymphotoxin. Science 1994;264:703-707.

20. Futterer A, Mink K, Luz A, Kosco-Vilbois MH, Pfeffer K: The lymphotoxin beta receptor controls organogenesis and affinity maturation in peripheral lymphoid tissues. Immunity 1998;9:59-70.

21. Taylor RT, Lugering A, Newell KA, Williams IR: Intestinal cryptopatch formation in mice requires lymphotoxin alpha and the lymphotoxin beta receptor. J Immunol 2004;173:7183-7189.

22. Kaiserling E: Newly-formed lymph nodes in the submucosa in chronic inflammatory bowel disease. Lymphology 2001;34:22-29.

23. Mackay F, Browning JL, Lawton P, Shah SA, Comiskey M, Bhan AK, Mizoguchi E, Terhorst C, Simpson SJ: Both the lymphotoxin and tumor necrosis factor pathways are involved in experimental murine models of colitis. Gastroenterology 1998;115:1464-1475.

24. Melgar S, Karlsson A, Michaelsson E: Acute colitis induced by dextran sulfate sodium progresses to chronicity in C57BL/6 but not in BALB/c mice: correlation between symptoms and inflammation. Am J Physiol Gastrointest Liver Physiol 2005;288:G1328-G1338.

25. Okayasu I, Hatakeyama S, Yamada M, Ohkusa T, Inagaki Y, Nakaya R: A novel method in the induction of reliable experimental acute and chronic ulcerative colitis in mice. Gastroenterology 1990;98:694-702.

26. Kitajima S, Takuma S, Morimoto M: Changes in colonic mucosal permeability in mouse colitis induced with dextran sulfate sodium. Exp Anim 1999;48:137-143.

27. Vondenhoff MF, Greuter M, Goverse G, Elewaut D, Dewint P, Ware CF, Hoorweg K, Kraal G, Mebius RE: LTbetaR signaling induces cytokine expression and up-regulates lymphangiogenic factors in lymph node anlagen. J Immunol 2009;182:5439-5445.

28. Gunn MD, Kyuwa S, Tam C, Kakiuchi T, Matsuzawa A, Williams LT, Nakano H: Mice lacking expression of secondary lymphoid organ chemokine have defects in lymphocyte homing and dendritic cell localization. J Exp Med 1999;189:451-460.

29. Luther SA, Tang HL, Hyman PL, Farr AG, Cyster JG: Coexpression of the chemokines ELC and SLC by T zone stromal cells and deletion of the ELC gene in the plt/plt mouse. Proc Natl Acad Sci U S A 2000;97:12694-12699.

30. Taylor RT, Patel SR, Lin E, Butler BR, Lake JG, Newberry RD, Williams IR: Lymphotoxin-independent expression of TNF-related activation-induced cytokine by stromal cells in cryptopatches, isolated lymphoid follicles, and Peyer's patches. J Immunol 2007;178:5659-5667.

31. Moyron-Quiroz JE, Rangel-Moreno J, Kusser K, Hartson L, Sprague F, Goodrich S, Woodland DL, Lund FE, Randall TD: Role of inducible bronchus associated lymphoid tissue (iBALT) in respiratory immunity. Nat Med 2004;10:927-934.